

## High Resolution Crystal Structure of the Methylcobalamin Analogues Ethylcobalamin and Butylcobalamin by X-ray Synchrotron Diffraction

Luciana Hannibal,<sup>†,‡</sup> Clyde A. Smith,<sup>§</sup> Jessica A. Smith,<sup>§</sup> Armend Axhemi,<sup>†</sup> Abby Miller,<sup>||</sup> Sihe Wang,<sup>||</sup> Nicola E. Brasch,<sup>†,‡</sup> and Donald W. Jacobsen<sup>\*,†,‡,||,¶</sup>

<sup>†</sup>Department of Cell Biology, Lerner Research Institute, Cleveland Clinic, Cleveland, Ohio 44195, <sup>‡</sup>School of Biomedical Sciences, Kent State University, Kent, Ohio 44242, <sup>§</sup>Stanford Synchrotron Radiation Laboratory, Stanford University, Menlo Park, California 94025, <sup>||</sup>Department of Clinical Pathology, Cleveland Clinic, Cleveland, Ohio 44195, <sup>⊥</sup>Department of Chemistry, Kent State University, Kent, Ohio 44242, and <sup>¶</sup>Department of Molecular Medicine, Cleveland Clinic Lerner College of Medicine, Case Western Reserve University, Cleveland, Ohio 44106

Received March 26, 2009

The X-ray crystal structures of the methylcobalamin (MeCbl) analogues ethylcobalamin (EtCbl) and butylcobalamin (BuCbl) are reported. The X-ray crystal structures of EtCbl and BuCbl were obtained with some of the lowest crystallographic residuals ever achieved for cobalamins ( $R = 0.0468$  and  $0.0438$ , respectively). The Co–C bond distances for EtCbl and BuCbl are 2.023(2) and 2.028(4) Å, whereas the Co– $\alpha$ -5,6-dimethylbenzimidazole (Co–N3B) bond distances were 2.232(1) and 2.244(1) Å, respectively. Although EtCbl and BuCbl displayed a longer Co–N3B bond than that observed in the naturally occurring methylcobalamin, the orientation of the  $\alpha$ -5,6-dimethylbenzimidazole moiety with respect to the corrin ring did not vary substantially among the structures. The lengthening of both Co–C and Co–N3B bonds in EtCbl and BuCbl can be attributed to the “inverse” *trans* influence exerted by the  $\sigma$ -donating alkyl groups, typically observed in alkylcobalamins. Analysis of the molecular surface maps showed that the alkyl ligands in EtCbl and BuCbl are directed toward the hydrophobic side of the corrin ring. The corrin fold angles in EtCbl and BuCbl were determined to be  $14.7^\circ$  and  $13.1^\circ$ , respectively. A rough correlation exists between the corrin fold angle and the length of the Co–N3B bond, and both alkylcobalamins follow the same trend.

### Introduction

Cobalamins are cobalt complexes coordinated by four equatorial nitrogens from a corrin ring macrocycle. The corrin ring incorporates a total of seven amide side chains, three acetamides and four propionamides (Figure 1). In addition, the Co center is coordinated to a nitrogen atom from a 5,6-dimethylbenzimidazole (DMB) moiety at the lower ( $\alpha$ ) axial position. Cleavage of the DMB moiety from Cbl generates the “base-off” conformation of the complex. The upper ( $\beta$ ) axial position can be occupied by a range of ligands including alkyl groups such as methyl and 5'-deoxyadenosyl, giving rise to the naturally occurring organometallic corrinoids methylcobalamin (MeCbl) and adenosylcobalamin (AdoCbl), respectively. The first evidence for the existence of a naturally occurring organometallic compound was presented by Lenhert and Hodgkin in 1961, with the elucidation of the structure of AdoCbl by X-ray crystallography.<sup>1</sup> The analysis revealed the presence of a Co–C bond linking the 5'-deoxyadenosyl moiety with the cobalt center of cobalamin. In 1985, the X-ray

crystal structure of MeCbl was reported, showing once again the presence of a Co–C bond.<sup>2</sup>

Organometallic corrinoids serve as important cofactors and methyl transfer catalysts in enzymatic reactions, in both prokaryotes and eukaryotes.<sup>3,4</sup> AdoCbl-dependent enzymes catalyze rearrangement reactions in which a key step involves Co–C bond homolysis to produce an adenosyl radical and cob(II)alamin.<sup>5,6</sup> MeCbl-dependent methionine synthases catalyze the remethylation of homocysteine to methionine, generating cob(I)alamin in the process. The latter is remethylated by *N*<sup>5</sup>-methyl-tetrahydrofolate to form MeCbl and tetrahydrofolate. Thus, in contrast to AdoCbl-dependent reactions, MeCbl-dependent methionine synthases formally operate via heterolytic cleavage of the Co–C bond.<sup>6,7</sup>

(2) Rossi, M.; Glusker, J. P.; Randaccio, L.; Summers, M. F.; Toscano, P. J.; Marzilli, L. G. *J. Am. Chem. Soc.* **1985**, *107*, 1729–1738.

(3) Banerjee, R.; Chowdhury, S. Methylmalonyl-CoA mutase. In *Chemistry and Biochemistry of B12*; Wiley-IEEE: New York, 1999; p 921.

(4) Matthews, R. G. Cobalamin-dependent methionine synthase. In *Chemistry and Biochemistry of B12*; Wiley-IEEE: New York, 1999; p 921.

(5) Banerjee, R. V.; Matthews, R. G. *FASEB J.* **1990**, *4*, 1450–1459.

(6) Ludwig, M. L.; Matthews, R. G. *Annu. Rev. Biochem.* **1997**, *66*, 269–313.

(7) Banerjee, R.; Ragsdale, S. W. *Annu. Rev. Biochem.* **2003**, *72*, 209–247.

\*To whom correspondence should be addressed. E-mail: jacobsd@ccf.org.

(1) Lenhert, P. G.; Hodgkin, D. C. *Nature* **1961**, *192*, 937–938.

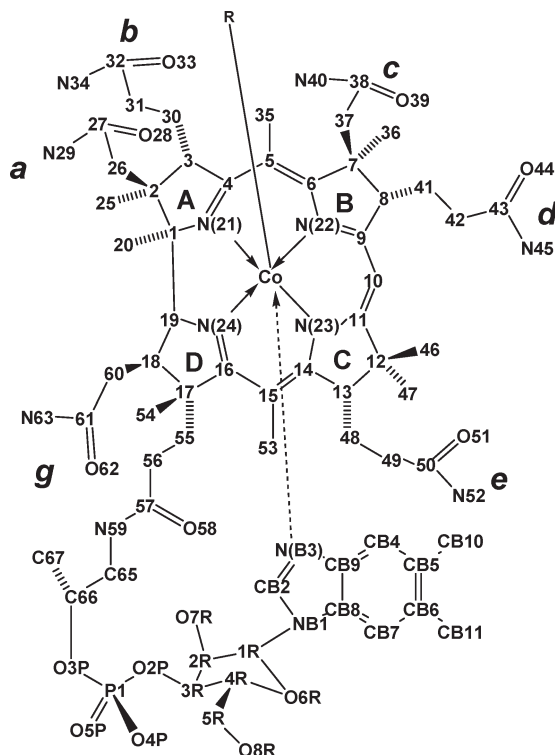


**Figure 1.** Chemical structure of cobalamins with atom numbering.

Interestingly, MeCbl-dependent methionine synthases are inactivated *in vitro* upon incubation with alkylating agents. This inactivation is reversed by photolysis, which suggests the formation of a non-functional alkylcobalamin (that is, a MeCbl analogue) in the enzyme's active site.<sup>8–10</sup> More recently, Yamada and co-workers showed that rat methionine synthase, which requires MeCbl for its catalytic activity, forms inactive complexes with EtCbl and propylcobalamin (PrCbl).<sup>11</sup> Again, the enzymatic activity was restored upon exposure to light. Hence, the enzymatic reaction appeared to be very sensitive to nature of the ligand coordinating at the upper axial position.

*In vivo*, cyanocobalamin (CNCbl, vitamin B<sub>12</sub>) is converted to MeCbl and AdoCbl in both pro- and eukaryotes.<sup>7,12</sup> Randaccio and co-workers have recently redetermined the X-ray crystal structures of AdoCbl, MeCbl, and CNCbl using synchrotron diffraction.<sup>13,14</sup> Analysis of the crystal structures of AdoCbl,<sup>1</sup> MeCbl,<sup>2</sup> and CNCbl<sup>14</sup> showed that the Co–C bond in MeCbl has a strength similar to that of AdoCbl, but it is significantly weaker than that in CNCbl.<sup>13</sup> The rate of cleavage of the Co–C bond in several alkylcobalamins including the natural cofactors is strongly influenced by structural, electronic and solvent factors.<sup>15</sup> Indeed,

R	Compound
H <sub>2</sub> O	Aquacobalamin
CN <sup>−</sup>	Cyanocobalamin
5'-deoxyadenosyl	Adenosylcobalamin
CH <sub>3</sub>	Methylcobalamin
CH <sub>3</sub> CH <sub>2</sub>	Ethylcobalamin
CH <sub>3</sub> (CH <sub>2</sub> ) <sub>2</sub>	Butylcobalamin

density functional theory (DFT) calculations for alkylcorrinoids indicate that weakening of the lower  $\alpha$ -Co–N(DMB) bond (*trans* influence) is important for achieving a low-energy pathway in the electron transfer mechanism of the Co–C bond breaking in alkylcobalamins.<sup>13</sup> In addition, DFT studies also suggest that the length of the Co–N3B bond is largely influenced by crystal packing forces.<sup>16</sup> This is particularly relevant to alkylcobalamins incorporating bulky upper axial ligands, such as the 5'-deoxyadenosyl ligand in AdoCbl, which is capable of establishing hydrogen bonding and van der Waals interactions with the neighboring atoms, but of less importance for alkylcobalamins possessing small upper axial ligands (like methyl in MeCbl) for which interactions with the rest of the atoms are essentially impeded.<sup>17</sup>

Another important aspect of alkylcobalamin chemistry has emerged from several studies where cobalamins operate as catalysts in the dechlorination of perchloro- and trichloroethylene,<sup>18–20</sup> which are widespread contaminants of soils and aquifers.<sup>21–23</sup> The process by which these toxic species are converted to ethylene and acetylene takes place *in vivo* in certain strains of bacteria<sup>24,25</sup> and involves corrinoid-dependent

(8) Burke, G. T.; Mangum, J. H.; Brodie, J. D. *Biochemistry* **1971**, *10*, 3079–3085.

(9) Taylor, R. T.; Weissbach, H. *J. Biol. Chem.* **1967**, *242*, 1509–1516.

(10) Taylor, R. T.; Whitfield, C.; Weissbach, H. *Arch. Biochem. Biophys.* **1968**, *125*, 240–252.

(11) Yamada, K.; Yamada, S.; Tobimatsu, T.; Toraya, T. *J. Biol. Chem.* **1999**, *274*, 35571–35576.

(12) Banerjee, R. *Chem Biol* **1997**, *4*, 175–186.

(13) Ouyang, L.; Rulis, P.; Ching, W. Y.; Nardin, G.; Randaccio, L. *Inorg. Chem.* **2004**, *43*, 1235–1241.

(14) Randaccio, L.; Furlan, M.; Geremia, S.; Slouf, M.; Srnova, I.; Toffoli, D. *Inorg. Chem.* **2000**, *39*, 3403–3413.

(15) Birke, R. L.; Huang, Q.; Spataru, T.; Gosser, D. K., Jr. *J. Am. Chem. Soc.* **2006**, *128*, 1922–1936.

(16) Rovira, C.; Kozłowski, P. M. *J. Phys. Chem. B* **2007**, *111*, 3251–3257.

(17) Rovira, C.; Biarnes, X.; Kunc, K. *Inorg. Chem.* **2004**, *43*, 6628–6632.

(18) Hatfield, K.; Deng, B.; Burris, D. R.; Buck, L. E.; Delcomyn, C. A. *Environ. Toxicol. Chem.* **1998**, *17*, 1681.

(19) McCauley, K. M.; Pratt, D. A.; Wilson, S. R.; Shey, J.; Burkey, T. J.; van der Donk, W. A. *J. Am. Chem. Soc.* **2005**, *127*, 1126–1136.

(20) Pratt, D. A.; van der Donk, W. A. *J. Am. Chem. Soc.* **2005**, *127*, 384–396.

(21) Magara, Y.; Furuichi, T. *Dev. Toxicol. Environ. Sci.* **1986**, *12*, 231–243.

(22) McLaughlin, J. K.; Blot, W. J. *Int. Arch. Occup. Environ. Health* **1997**, *70*, 222–231.

(23) Squillace, P. J.; Moran, M. J.; Lapham, W. W.; Price, C. V.; Clawges, R. M.; Zogorski, J. S. *Environ. Sci. Technol.* **1999**, *33*, 4176–4187.

(24) Holliger, C.; Hahn, D.; Harmsen, H.; Ludwig, W.; Schumacher, W.; Tindall, B.; Vazquez, F.; Weiss, N.; Zehnder, A. J. *Arch. Microbiol.* **1998**, *169*, 313–321.

(25) Holliger, C.; Wohlfarth, G.; Diekert, G. *FEMS Microbiol. Rev.* **1998**, *22*, 383–397.

enzymes. Model studies indicate that the reactions involve breaking and forming of the corrinoid Co–C bond.<sup>18–20</sup> The X-ray crystal structures of two model catalysts, vinylcobalamin and *cis*-chlorovinylcobalamin, were recently reported.<sup>19</sup>

Herein, we report the high-resolution X-ray crystal structure of ethylcobalamin (EtCbl) and butylcobalamin (BuCbl). Both analogues displayed the so-called “inverse” *trans* influence, typically observed in alkylcobalamins. Analysis of the electronic surface maps indicate that both the ethyl and the butyl ligands are directed toward the hydrophobic side of the cobalamin molecule. This particular conformation has been observed in other Co–C bonded cobalamins and appears to be an important feature of cofactor reactivity *in vivo*.<sup>26</sup>

## Experimental Section

**General Procedures and Chemicals.** Hydroxocobalamin hydrochloride (HOCbl·HCl) was purchased from Fluka. Stated purity by manufacturer is  $\geq 96\%$ . However, the aromatic region of the <sup>1</sup>H NMR spectrum shows it contains at least  $\sim 6\%$  impurities.<sup>27</sup> Alkyl halides (bromoethane, 99%, FW 108.97, d 1.46 g/mL, and 1-bromobutane, 99%, FW 137.02, d 1.276 g/mL) were purchased from Sigma. All chemicals were used without further purification. Water was purified using a Barnstead Nanopure Diamond water purification system and/or HPLC grade water was used. All solutions used for the synthesis of the alkylcobalamins were degassed by at least three freeze–pump–thaw cycles under argon using standard Schlenck techniques. Syntheses were carried out in an MBraun Labmaster 130(1250/78) glovebox operating under argon atmosphere, or in an anaerobic cuvette with continuous argon bubbling. Both synthesis and handling of the alkylcobalamins were performed in the darkness under red-dim light illumination.

UV–visible spectra were recorded on a Cary 5000 spectrophotometer equipped with a thermostatted cell holder, operating with WinUV Bio software (version 3.00). <sup>1</sup>H NMR spectra were recorded on a Varian Inova 500 MHz spectrometer equipped with a 5 mm thermostatted (22.0  $\pm$  0.5 °C) probe. Solutions were prepared in D<sub>2</sub>O and TSP (3-(trimethylsilyl)propionic-2,2,3,3-d<sub>4</sub> acid, Na<sup>+</sup> salt) used as an internal reference. pH measurements were made at room temperature with a Corning Model 445 pH meter equipped with a Mettler-Toledo Inlab 423 electrode.

Liquid chromatography electrospray ionization mass spectrometry (LC-ESI-MS) was carried out using a Thermo Finnigan Triple Stage Quadrupole (TSQ) Quantum Ultra mass spectrometer (Thermo Electron Corporation, Waltham, MA, USA). Each alkylcobalamin was dissolved in 95% MeOH/5% H<sub>2</sub>O at a concentration of 10 mg/L and infused at a rate of 10  $\mu$ L/min.

**Synthesis of Alkylcobalamins.** EtCbl and BuCbl were synthesized by reacting cob(I)alamin with the corresponding alkyl halide for  $\sim 10$  min in the absence of light under anaerobic conditions according to literature methods.<sup>28,29</sup> In both cases, cob(I)alamin was generated by reduction of aquacobalamin with 10 equiv of sodium borohydride (NaBH<sub>4</sub>). Prior to adding the alkyl halide, excess NaBH<sub>4</sub> was destroyed by the addition of a small excess of anaerobic acetone. The alkylcobalamin product precipitated upon dropwise addition into cold acetone (4 °C, 20 mL) and was filtered and dried overnight under vacuum at 60 °C. Alkyl halides are soluble in acetone; hence it is unlikely that unreacted alkyl halide co-precipitates with the product. The percentage of non-cobalamin impurities was determined by

converting the products to dicyanocobalamin, (CN)<sub>2</sub>Cbl<sup>−</sup> (0.10 M KCN, pH 10.0,  $\epsilon_{368} = 3.04 \times 10^4 \text{ M}^{-1} \text{ cm}^{-1}$ ).<sup>30</sup>

**EtCbl.** Bromoethane (5 equiv,  $1.27 \times 10^{-4}$  mol, 9.5  $\mu$ L) was added to HOCbl·HCl (35 mg,  $2.53 \times 10^{-5}$  mol) dissolved in H<sub>2</sub>O (1.0 mL). Yield:  $\sim 90\%$ . <sup>1</sup>H NMR (D<sub>2</sub>O,  $\delta$ , ppm): 6.06, 6.26, 6.27, 7.00, and 7.18;  $\sim 98\%$  purity.<sup>27</sup> ES/MS (+ve), *m/z*: 1358.8 (calcd for [EtCbl + H]<sup>+</sup>, C<sub>64</sub>H<sub>94</sub>N<sub>13</sub>O<sub>14</sub>PCo = 1358.6); 1380.7 (calcd for [EtCbl + Na]<sup>+</sup>, C<sub>64</sub>H<sub>93</sub>N<sub>13</sub>O<sub>14</sub>PCoNa = 1380.6); 1381.6 (calcd for [EtCbl + H + Na], C<sub>64</sub>H<sub>94</sub>N<sub>13</sub>O<sub>14</sub>PCoNa = 1381.6); 680.0 (calcd for [EtCbl + 2H]<sup>2+</sup>, C<sub>64</sub>H<sub>95</sub>N<sub>13</sub>O<sub>14</sub>PCo = 679.8).

**BuCbl.** 1-Bromobutane (5 equiv,  $1.27 \times 10^{-4}$  moles, 13.6  $\mu$ L) was added to HOCbl·HCl (35 mg,  $2.53 \times 10^{-5}$  mol) dissolved in H<sub>2</sub>O (1.0 mL). Yield:  $\sim 87\%$ . <sup>1</sup>H NMR (D<sub>2</sub>O,  $\delta$ , ppm): 6.08, 6.26, 6.29, 7.01, and 7.18;  $\sim 98\%$  purity.<sup>27</sup> ES/MS (+ve), *m/z*: 1386.7 (calcd for [BuCbl + H]<sup>+</sup>, C<sub>66</sub>H<sub>98</sub>N<sub>13</sub>O<sub>14</sub>PCo = 1386.6); 1408.7 (calcd for [BuCbl + Na]<sup>+</sup>, C<sub>66</sub>H<sub>97</sub>N<sub>13</sub>O<sub>14</sub>PCoNa = 1408.6); 1409.8 (calcd for [BuCbl + H + Na], C<sub>66</sub>H<sub>98</sub>N<sub>13</sub>O<sub>14</sub>PCoNa = 1409.6) 693.9 (calcd for [BuCbl + 2H]<sup>2+</sup>, C<sub>66</sub>H<sub>99</sub>N<sub>13</sub>O<sub>14</sub>PCo = 693.8).

**X-ray Diffraction Studies.** With the aim of obtaining suitable crystals of structural analogues of MeCbl, we synthesized and crystallized EtCbl and BuCbl. The synthesis of propylcobalamin (PrCbl), pentylcobalamin (PnCbl), and hexylcobalamin (HxCbl) was also carried out, but attempts to obtain crystals of these derivatives were unsuccessful.

Crystals of EtCbl and BuCbl were grown from their corresponding synthesis mixtures, at room temperature, under anaerobic conditions. Crystals suitable for X-ray analysis appeared after 1 week. The EtCbl and BuCbl crystals were transferred into paratone oil, and any residual synthesis mixture was carefully removed by dragging the crystals through the oil. The crystals were then mounted in thin nylon loops on copper magnetic pins (Hampton Research) and flash-cooled in liquid nitrogen. X-ray diffraction experiments were carried out at beamline BL9–2 at the Stanford Synchrotron Radiation Laboratory (SSRL). Data from both complexes were collected on a MarMosaic 325 CCD detector using X-rays produced by a 16-pole wiggler insertion device through a flat Rh-coated collimating mirror, a liquid nitrogen-cooled double Si(111) crystal monochromator and a toroidal focusing mirror. The X-ray wavelength used for both crystals was 0.78468 Å (15800 eV). For EtCbl, two data sets were collected, both consisting of 360 0.5° images covering the same 180° angular range and with a crystal to detector distance of 95.0 mm. The first data set was recorded with an exposure time of 5 s and no beam attenuation, and the second data set had the same exposure time but the beam was attenuated by 75%. The two data sets were processed with the program XDS and scaled together with the program XSCALE.<sup>31</sup> Symmetry-equivalent and Bijvoet pairs were not merged and no absorption correction was applied. A total of 132135 reflections were measured, resulting in 18317 unique reflections to a nominal resolution of 0.71 Å, with a merging *R*-factor of 0.028 for common reflections on all images. For BuCbl only one data set was recorded comprising 360 0.5 images with an exposure time of 15 s and a crystal to detector distance of 95.0 mm. The data were processed and scaled with XDS and XSCALE,<sup>31</sup> with the symmetry-equivalent and Bijvoet pairs unmerged. A total of 66437 reflections were measured, giving a final unique data set of 20451 reflections to a resolution of 0.71 Å with a merging *R*-factor of 0.026.

Both structures were solved by Patterson methods as implemented in the program SHELXS.<sup>32</sup> The cobalt, phosphorus and some of the nitrogen atoms were readily located, the remainder

(26) Perry, C. B.; Marques, H. M. *S. Afr. J. Sci.* **2004**, *100*, 368–380.

(27) Brasch, N. E.; Finke, R. G. *J. Inorg. Biochem.* **1999**, *73*, 215–219.

(28) Kim, S. H.; Chen, H. L.; Feilchenfeld, N.; Halpern, J. *J. Am. Chem. Soc.* **1988**, *110*, 3120–3126.

(29) Pratt, J. M. *Inorganic chemistry of vitamin B12*; Academic Press Inc: New York, 1972; p 347.

(30) Barker, H. A.; Smyth, R. D.; Weissbach, H.; Toohey, J. I.; Ladd, J. N.; Volcani, B. E. *J. Biol. Chem.* **1960**, *235*, 480–488.

(31) Kabsch, W. *J. Appl. Crystallogr.* **1993**, *2*, 795–800.

(32) Sheldrick, G. M.; Schneider, T. R., SHELXL: High Resolution Refinement. In *Methods in Enzymology*; Sweet, R. M., Carter, C. W. J., Eds.; Academic Press: Orlando, FL, 1997; Vol. 277, pp 319–343.

of the lighter atoms later identified by difference Fourier synthesis. The structures were refined by full-matrix least-squares methods using SHELXL.<sup>32</sup> A correction for the anomalous scattering from cobalt at 15800 eV was applied during refinement. All non-hydrogen atoms were refined with anisotropic thermal parameters, and hydrogen atoms were added in idealized positions and refined in riding positions at the very end of the refinement. Additional difference electron density peaks were modeled as water molecules. Seventeen water molecules were added to the EtCbl structure and refined with full occupancy. Twenty water molecules were added to BuCbl, 10 with fractional occupancies. The final crystallographic *R* factor (*R*<sub>1</sub>) for EtCbl was 0.0468 for 18291 reflections with  $F_o > 4\sigma_F$ , and for BuCbl *R*<sub>1</sub> was 0.0438 for 20171 reflections with  $F_o > 4\sigma_F$ .

The CCDC database (EtCbl: CCDC 721275; BuCbl: CCDC 721276) contains the supplementary crystallographic data for this paper. These data can be obtained free of charge via www.ccdc.cam.ac.uk/data\_request/cif, by emailing data\_request@ccdc.cam.ac.uk, or by contacting The Cambridge Crystallographic Data Centre, 12, Union Road, Cambridge CB2 1EZ, U.K.; fax: +44 1223 336033.

## Results and Discussion

**Synthesis and Characterization of EtCbl and BuCbl.** The structural characterization of a number of corrinoid complexes has facilitated our understanding of cobalamin chemistry in vivo.<sup>33</sup> For example, comparison of the protein-bound cobalamins to model compounds have shown that the DMB side chain of ring D is displaced from Co in the protein structures of methionine synthase and methylmalonyl-CoA mutase, and some of the propionamide and acetamide side chains have reoriented to hydrogen-bond to protein atoms.<sup>34</sup> The plane of the histidine residues that bind Co are oriented similarly to the benzimidazole rings of the model cobalamins.<sup>34</sup> Upward folding of the corrin ring and strain induced alterations of the Co–C and Co–N axial bonds have been observed in the protein-bound structures compared to the protein-free MeCbl and AdoCbl X-ray structures.<sup>34</sup>

We recently reported the X-ray crystal structures of imidazolylcobalamin (ImCbl) and histidylcobalamin (HisCbl),<sup>35</sup> cobalamin models for aquacobalamin bound to the B<sub>12</sub> transporter transcobalamin.<sup>36,37</sup> A superposition of the model cobalamins with that of the protein-bound showed that the orientation of the imidazole with respect to the corrin ring is the same in the bound protein and in the isolated cobalamin.<sup>35,37</sup> The Co–N bond distances of the upper and lower axial ligands in the protein-bound cobalamin were considerable longer than those found in the model cobalamins, whereas the corrin fold angle was smaller in the protein-bound cobalamin compared to the corresponding protein-free form.<sup>35,37</sup>

The partial characterization of alkylcobalamins other than MeCbl has been previously reported by other laboratories and our UV–visible and <sup>1</sup>H NMR spectroscopic data

**Table 1.** UV-visible and <sup>1</sup>H NMR Spectroscopy Data<sup>a</sup>

Cobalamin	UV–visible wavelength maxima (nm)			chemical shifts (ppm)				
MeCbl	265, (318) <sup>b</sup> , 340, 377, 528	7.20	6.98	6.29	6.28	5.91		
EtCbl	265, 319, 349, (378), 513	7.18	7.00	6.27	6.26	6.06		
BuCbl	265, 319, 349, (378), 515	7.18	7.01	6.29	6.26	6.08		

<sup>a</sup> UV-visible measurements were performed in water, pH 6.80, at 25°C. <sup>1</sup>H NMR measurements were carried out in D<sub>2</sub>O, pD 7.5, at 25°C. <sup>b</sup> Shoulders are given in parentheses.

for EtCbl and BuCbl (Table 1) were in excellent agreement with the literature.<sup>29,38–40</sup> UV–vis and <sup>1</sup>H NMR spectra were almost identical for EtCbl and BuCbl and differed significantly from that of MeCbl (Table 1). The  $\gamma$ -band of the UV–visible spectrum of corrinoids, which is the most intense band in the near-ultraviolet region, reflects the amount of negative charge donated by the upper axial ligand to the cobalt via the  $\sigma$ -bond.<sup>29</sup> This was observed for EtCbl and BuCbl when compared to MeCbl (Table 1). On the other hand, the <sup>1</sup>H NMR resonance of the C10 hydrogen for EtCbl and BuCbl are considerably downfield compared with MeCbl (6.06 and 6.08 ppm, respectively, versus 5.91 ppm for MeCbl). The effect of the upper axial ligands of the Cbl on the hydrogen atom on C10, the bridge carbon between rings B and C (Figure 1) has been previously studied.<sup>29</sup> Examination of MeCbl, EtCbl, PrCbl, and BuCbl showed that strong electron donating ligands in the  $\beta$ -axial position of hexacoordinated corrinoids induced a downfield shift in the magnetic resonance of the C10 hydrogen.<sup>29</sup> Our results follow the same pattern (Table 1). Also, replacement of the C10 hydrogen by another substituent affects the electronic structure of the corrin macrocycle and influences the binding properties of the cobalt center.<sup>41–43</sup> These findings indicate that the hydrogen atom in C10 is extremely sensitive to its electronic environment and vice versa. Thus, the chemical shifts of the hydrogen in C10 for EtCbl and BuCbl display the correlation expected for the stronger electron donating ability of the respective alkyl ligands compared to that of the methyl group in MeCbl (Table 1).

**X-ray Structural Characterization of EtCbl and BuCbl.** Suitable crystals for X-ray analysis were obtained for EtCbl and BuCbl. Both EtCbl and BuCbl crystallized in the orthorhombic space group *P*2<sub>1</sub>2<sub>1</sub>2<sub>1</sub> with cell parameters 16.00 Å × 21.02 Å × 24.54 Å, and 16.03 Å × 20.73 Å × 24.62 Å, respectively. A summary of the crystallographic data and refinement parameters is presented in Table 2. The crystal structure and the crystal packing of the cobalamin molecule in this space group has been described exhaustively in the literature, and the current structures do not deviate markedly from the cobalamin structures known to date. The final *R*-factors of 0.0468 and 0.0438 for the two

(33) Randaccio, L.; Geremia, S.; Nardin, G.; Wuerger, J. *Coord. Chem. Rev.* **2006**, *250*, 1332–1350.

(34) Ludwig, M. L.; Evans, P. R. X-ray crystallography of B12 enzymes: methylmalonyl-CoA mutase and methionine synthase. In *Chemistry and Biochemistry of B12*; Wiley-IEEE: New York, 1999; p 921.

(35) Hannibal, L.; Bunge, S. D.; van Eldik, R.; Jacobsen, D. W.; Kratky, C.; Gruber, K.; Brasch, N. E. *Inorg. Chem.* **2007**, *46*, 3613–3618.

(36) Garau, G.; Fedosov, S. N.; Petersen, T. E.; Geremia, S.; Randaccio, L. *Acta Crystallogr., Sect. D: Biol. Crystallogr.* **2001**, *57*, 1890–1892.

(37) Wuerger, J.; Garau, G.; Geremia, S.; Fedosov, S. N.; Petersen, T. E.; Randaccio, L. *Proc. Natl. Acad. Sci. U.S.A.* **2006**, *103*, 4386–4391.

(38) Cole, A. G.; Yoder, L. M.; Shiang, J. J.; Anderson, N. A.; Walker, L. A. 2nd; Banaszak Holl, M. M.; Sension, R. J. *J. Am. Chem. Soc.* **2002**, *124*, 434–441.

(39) Taylor, R. T.; Smucker, L.; Hanna, M. L.; Gill, J. *Arch. Biochem. Biophys.* **1973**, *156*, 521–533.

(40) Smith, E. L.; Mervyn, L.; Muggleton, P. W.; Johnson, A. W.; Shaw, N. *Ann. N.Y. Acad. Sci.* **1964**, *112*, 565–574.

(41) Brown, K. L.; Cheng, S.; Zou, X.; Zubkowski, J. D.; Valente, E. J.; Knapton, L.; Marques, H. M. *Inorg. Chem.* **1997**, *36*, 3666–3675.

(42) Knapton, L.; Marques, H. M. *Dalton Trans.* **2005**, 889–895.

(43) Marques, H. M.; Knapton, L.; Zou, X.; Brown, K. L. *J. Chem. Soc., Dalton Trans.* **2002**, 3195–3200.

**Table 2.** Refinement Parameters for EtCbl and BuCbl

	EtCbl	BuCbl
empirical formula	C <sub>64</sub> H <sub>91</sub> N <sub>13</sub> O <sub>31</sub> CoP	C <sub>66</sub> H <sub>101</sub> N <sub>13</sub> O <sub>35</sub> CoP
H <sub>2</sub> O sites	17	21
formula weight	1628.40	1726.50
crystal system	orthorhombic	orthorhombic
space group	<i>P</i> 2 <sub>1</sub> 2 <sub>1</sub> 2 <sub>1</sub>	<i>P</i> 2 <sub>1</sub> 2 <sub>1</sub> 2 <sub>1</sub>
unit cell dimensions:		
<i>a</i> [Å]	16.00	16.03
<i>b</i> [Å]	21.02	20.73
<i>c</i> [Å]	24.54	24.62
<i>V</i> [Å <sup>3</sup> ]	8253.29	8181.27
<i>Z</i>	4	4
<i>D</i> <sub>calc</sub> [g cm <sup>-3</sup> ]	1.106	1.139
<i>μ</i> [mm <sup>-1</sup> ]	0.29	0.29
<i>F</i> (000)	2924	2988
crystal size [mm]	0.6 × 0.1 × 0.1	0.7 × 0.1 × 0.1
<i>θ</i> -range for data collection [deg]	67.1	67.0
temperature [K]	100	100
wavelength [Å]	0.78468	0.78468
no. of unique reflections	18317	20414
no. of reflections with <i>I</i> > 4 $\sigma$ <sub>1</sub>	18291	20171
<i>R</i> (int)	0.0281	0.0262
data/restraints/parameters	18317/0/1037	20414/183/1136
GOF on <i>F</i> <sup>2</sup>	1.046	0.769
final <i>R</i> indices:		
<i>R</i> <sub>1</sub> ( <i>I</i> > 4 $\sigma$ <sub>1</sub> /all data)	0.0468/0.0469	0.0438/0.0443
<i>wR</i> <sub>2</sub> (all data)	0.1308	0.1249
largest diff. peak/hole [e/Å <sup>-3</sup> ]	0.88/−1.11	0.85/−0.49

structures are among the lowest ever achieved for cobalamin structures, and this can be directly correlated with the quality of the diffraction data. The merging *R*-factors for the synchrotron data were extremely good (0.0281 and 0.0262 for the symmetry-related reflections) and the average signal-to-noise values (*I*/ $\sigma$ ) were 57.2 and 31.4 for EtCbl and BuCbl, respectively. Comparison of the two data sets indicates that although they both extend to approximately the same resolution (around 0.71 Å), the EtCbl data is almost twice as strong as the BuCbl data (as judged by the *I*/ $\sigma$  values quoted above). Despite the fact that the data resulted from two data sets merged together, the better signal-to-noise ratio clearly results in a more accurately determined crystal structure.

The crystal packing of the cobalamin molecule in the *P*2<sub>1</sub>2<sub>1</sub>2<sub>1</sub> space group is generally analyzed by comparison of the ratios of the *c/a* and *b/a* unit cell dimensions.<sup>44</sup> The EtCbl ratios of *c/a* = 1.534 and *b/a* = 1.314, and the BuCbl ratios of *c/a* = 1.536 and *b/a* = 1.293 indicate that these crystals are typical of cluster I packing.<sup>44</sup> Cobalamins that belong to the same crystal packing type display remarkably similar conformations of their side chains, as well as a similar pattern of intra- and intermolecular hydrogen bonding.<sup>14</sup> The cobalamin molecules are oriented in the crystal such that the plane of the corrin ring is almost parallel to the *ab* plane of the unit cell, tilted by approximately 5–10°, and when viewed down the *a*-axis, the molecules appear to adopt a slight zigzag sheet-like pattern because of this tilt, running parallel to the *ab* plane. Layers of solvent molecules lie between the tilted cobalamin sheets, with the axial base and the upper

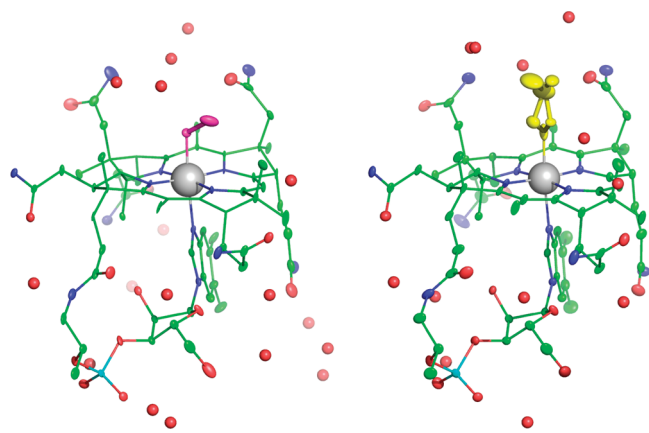


**Figure 2.** Thermal ellipsoid plots of EtCbl (left) and BuCbl (right). The ethyl  $\beta$ -axial ligand in EtCbl is shown in magenta and the butyl ligand (two conformations) in BuCbl is shown in yellow. The rest of the cobalamin complex is colored green (C), red (O), blue (N), and cyan (P). The cobalt in each case is shown as a gray sphere. The thermal ellipsoids were drawn at 75% probability for all the atoms except for the cobalt and the water molecules (shown as red spheres).

axial ligand projecting into this layer. Long solvent channels are also evident when viewed down the *c* axis. In both cases the solvent was modeled very accurately, with 17 placed in EtCbl and 20 in BuCbl, with the residual peaks in the electron density less than 1 e/Å<sup>3</sup> in both structures. Thermal ellipsoids plots for EtCbl and BuCbl (drawn at 75% probability) are presented in Figure 2. Of the 21 water molecules in the BuCbl structure, five were in fully occupied positions and the rest were refined with partial occupancy, initially set at 0.5 based upon the observed increase in their anisotropic displacement parameters when refined with full occupancy. Conversely, all 17 water molecules in the EtCbl structure were at fully occupied positions. In the two structures, all the water molecules are in hydrogen bonding contact with either oxygen or nitrogen atoms on the cobalamin moiety, or with other water molecules.

The conformation of the corrin ring is generally quantified by the fold angle around the Co–C10 axis, between the planes of the conjugated ring systems (plane 1: N21, C4, C5, C6, N22, C9, C10 and plane 2: N24, C16, C15, C14, N23, C11, C10; see Figure 1). In EtCbl and BuCbl this corrin fold angle is 14.8° and 13.2° respectively, the direction of the fold being toward the  $\beta$  face of the corrin (away from the  $\alpha$ -5,6-dimethylbenzimidazole group). The corresponding values for a number of other alkylcobalamins are given in Table 3. Recently, van der Donk and co-workers reported the X-ray structure of *cis*-chlorovinylcobalamin and vinylcobalamin.<sup>19</sup> Interestingly, *cis*-chlorovinylcobalamin exhibited a fold angle of 5.7 (9)° which is the smallest reported value for cobalamins (others fall in the 13.3° (AdoCbl) to 18.7° (H<sub>2</sub>OCbl<sup>+</sup>) range).<sup>19</sup> The authors attributed this result to interactions between the chlorine and the corrin ring and its  $\beta$ -substituents on the tetrapyrrolic macrocycle.<sup>19</sup> It was originally proposed that the extent of folding of the corrin ring was inversely related to the steric bulk of the  $\beta$ -axial ligand but it is now generally believed that the *trans* influence of the ligand is the critical factor.<sup>14,33</sup> There is a rough correlation between the corrin fold angle and the length of the Co–NB3 bond<sup>33</sup> (Figure 3). Although there

(44) Garau, G.; Geremia, S.; Marzilli, L. G.; Nardin, G.; Randaccio, L.; Tauzher, G. *Acta Crystallogr., Sect. B* 2003, 59, 51–59.

**Table 3.** Comparison of the Co Coordination Sphere in EtCbl, BuCbl, and Other Alkylcobalamin Complexes<sup>a</sup>

Cobalamin	Co–X (Å)	Co–N3B (Å)	fold angle (deg)	reference
EtCbl	2.023(2)	2.232(1)	14.8	this work
BuCbl	2.028(4)	2.244(1)	13.2	this work
MeCbl	1.979(4)	2.162(4)	14.7	14
AdoCbl	2.033(4)	2.237(3)	15.9	13
AdoCbl (neutron)	2.023(10)	2.214(9)	13.3	46
AdePrCbl	1.959(10)	2.212(8)	10.9	47
CNCbl	1.885(4)	2.041(3)	18.7	14
CHF <sub>2</sub> Cbl	1.949(7)	2.187(7)	15.6	48
CF <sub>3</sub> Cbl	1.878(12)	2.047(10)	15.6	49
vinylCbl	1.911(7)	2.165(6)	12.5(2)	19
<i>cis</i> -chlorovinylCbl	1.951(7)	2.144(5)	5.7 (9)	19
isoamylCbl	2.044(3)	2.277(2)	10.6	50
<i>R</i> -2,3-dihydroxypropylCbl	2.002(23)	2.269	10.6	51
<i>S</i> -2,3-dihydroxypropylCbl	2.079(30)	2.367	13.0	51

<sup>a</sup> Values are also given for CNCbl.

is considerable scattering, the parameters obtained for EtCbl and BuCbl are similar to those reported for AdoCbl structures (Figure 3). The Co–C bond distances in the two complexes are 2.023(2) Å and 2.028(4) Å for EtCbl and BuCbl, respectively. These distances are comparable to other Co–C bond lengths observed in cobalamin complexes (Table 3). In the EtCbl complex, the second carbon atom (C72) is directed away from the two amide groups which project up from the  $\beta$  face of the corrin at carbons C2 and C7, and points almost directly toward the C46 methyl group (attached to carbon C12 of the corrin, see Figure 1). This results in a Co–C71–C72 angle of 117.5°. By calculating a plane through the cobalt atom, C71 and C46, the degree of rotation of the C72 carbon out of this plane can be estimated at approximately 5°. In the BuCbl complex, two orientations of the butyl group were observed in the electron density, as presented in Figure 4. The first and third carbon atoms of both conformations were in identical positions, with the second and fourth carbon atoms occupying two distinct positions. The net effect is a rotation of the butyl group about an axis running between the first and third carbon atoms. The butyl group in both orientations is in a typical elongated conformation, also directed toward the hydrophobic side of the corrin ring similar to the ethyl group (Figure 4). However, neither of the two conformations of the butyl group have the C72 carbon atom in the same position as in the ethyl group with the C72 atoms rotated by approximately 29° and 62°, respectively, from the Co–C71–C46 plane. The Co–C71–C72 angles in the two conformations are 119.0 and 119.6°.

Analysis of other cobalamin complexes containing a Co–C bond (AdoCbl, vinylCbl, chlorovinylCbl) shows a similar pattern with the upper axial ligand directed toward the hydrophobic side of the  $\beta$  face of the corrin ring,

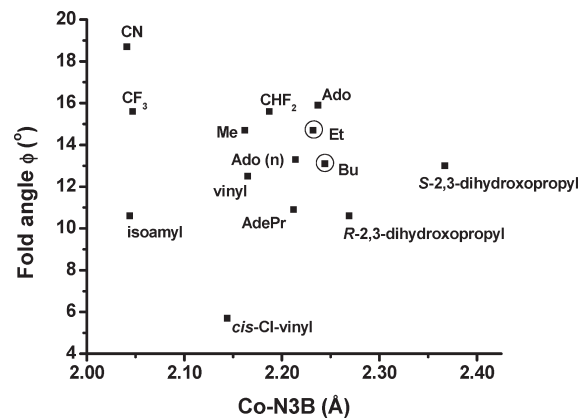


**Figure 3.** Scatter plot of the corrin fold angle ( $\phi$ ) versus the axial Co–N3B distance for Co–C bonded cobalamins. EtCbl and BuCbl are indicated with circled dots.

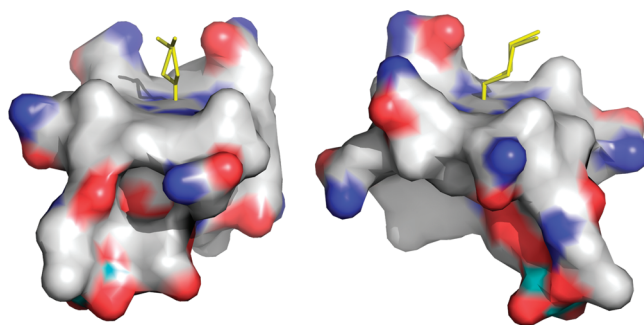


**Figure 4.** Molecular surface representations of BuCbl in two different orientations. The butyl group is directed toward the hydrophobic side of the corrin ring, similar to the ethyl group in EtCbl.

between the C46 methyl and the C54 methyl groups. In vinyl- and chlorovinylcobalamin, the former, possessing a similar steric bulk to that of EtCbl, the second carbon is rotated almost 49° toward the C54 methyl.<sup>19</sup> The four independent molecules in the asymmetric unit of the chlorovinylcobalamin complex show a range of values from 29° to 44° from the Co–C71–C46 plane. Adenosylcobalamin shows the largest rotation from this plane of almost 84°, which has the C atoms of the ribose moiety pointed almost directly at the C54 methyl group. Consequently, there appears to be no correlation between the size or the substituents on the second carbon atom and the direction in which the ligand points. Extending the analysis to other cobalamin complexes including those with Co–N, Co–O, and Co–S bonds showed that in all cases the substituent is directed toward this side of the corrin ring with a mean rotation from the Co–C71–C46 plane of approximately 44°, which bisects almost exactly the angular spread between the C46 and C54 methyl groups (87°). In fact, the 15° variation observed in the four chlorovinylcobalamin molecules<sup>19</sup> would indicate a large energy minimum delineated by the C46 and C54 methyl groups and dominated primarily by the hydrophobicity of this side of the corrin ring and the lack of any ordered hydrogen-bonded water molecules. Importantly, it has been proposed that the methyl groups on C46 and C54 and the methylene groups in side chains *a* and *c* protect the reactive methyl or adenosyl groups in the coenzymes during catalytic turnover<sup>26</sup> (see also references therein).

(45) Stubbe, J. *Science* **1994**, *266*, 1663–1664.

(46) Lenhert, P. G. *Proc. R. Soc. London, Ser. A* **1968**, *A303*, 45–84.

(47) Pagano, T. G.; Marzilli, L. G.; Flocco, M. M.; Tsai, C.; Carrell, H. L.; Glusker, J. P. *J. Am. Chem. Soc.* **1991**, *113*, 531–542.

(48) Wagner, T.; Afshar, C. E.; Carrell, H. L.; Glusker, J. P.; Englert, U.; Hogenkamp, H. P. *Inorg. Chem.* **1999**, *38*, 1785–1794.

(49) Zou, X.; Brown, K. L. *Inorg. Chim. Acta* **1998**, *267*, 305–308.

(50) Perry, C. B.; Fernandes, M. A.; Marques, H. M. *Acta Crystallogr., Sect. C* **2004**, *60*, m165–7.

(51) Alcock, N. W.; Dixon, R. M.; Golding, B. T. *J. Chem. Soc., Chem. Commun.* **1985**, 603–605.

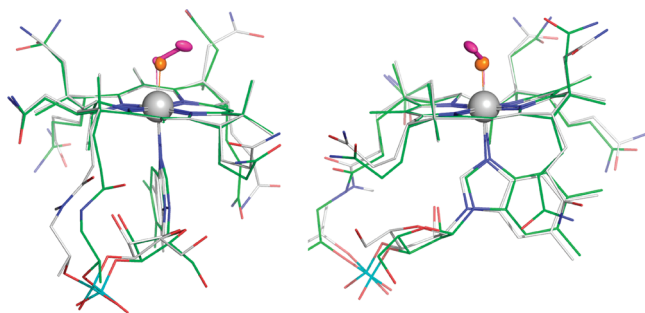


**Figure 5.** Superposition of the structures of MeCbl and EtCbl. Two approximately perpendicular views are shown. The methyl group is shown in orange and the ethyl group in magenta.

A superposition of the structure of EtCbl with that of the naturally occurring MeCbl is shown in Figure 5. There is high structural similarity among the structures as expected. The positions of the carbon atoms are visually similar in both complexes. However, a clear distinction of the two alkylcobalamins was possible by direct superposition of the two structures. Although the Co–N3B bond is significantly longer in EtCbl (2.232(1) Å) compared to MeCbl (2.162(4) Å), the orientation of the  $\alpha$ -5,6-dimethylbenzimidazole moiety with respect to the corrin ring is the same in both complexes.

There are seven amide side chains incorporated in the corrin ring. Three short acetamide side chains (*a*, *c*, and *g*), which project above the plane of the corrin and four propionamide (*b*, *d*, *e*, and *f*) side chains which extend below the plane of the corrin ring. An analysis of the amide side chains of 13 cobalamin structures performed by Perry et al. suggested that there is remarkable consistency in the conformation of the side chains among cobalamin structures, although side chains *c*, *d*, and *e* display greater flexibility with respect to *a*, *b*, *g*, and *f* side chains.<sup>26</sup> However, a more extensive examination of all the cobalamin structures elucidated in the last 20 years reported by Randaccio et al.,<sup>14</sup> showed that chains *a* and *d* assume very similar conformations in all structures, chain *g* appears in only two distinct conformations, whereas the other side chains display a large conformational freedom.<sup>14</sup> The analysis confirmed that in general, cobalamins belonging to the same cluster type display a similar conformation of their side chains.<sup>14,33</sup> EtCbl and BuCbl belong to cluster type I, which includes CNCbl·KCl, (NH<sub>2</sub>)<sub>2</sub>CSCbl, HOCbl, (*R*)-2,3-dihydroxopropylCbl and (*S*)-2,3-dihydroxopropylCbl and CNCbl (dry). In agreement with the literature,<sup>14</sup> the overall conformation of the side chains in EtCbl and BuCbl does not differ from that observed in other cobalamins in the same cluster, except for (NH<sub>2</sub>)<sub>2</sub>CSCbl. Figure 6 shows a superposition of the structures of EtCbl and (NH<sub>2</sub>)<sub>2</sub>CSCbl. Side chains *b*, *e*, *g*, and *f* showed similar conformations, whereas side chains *a*, *c*, and to a lesser extent *d*, differed in both structures.

The superposition of the structures of MeCbl and EtCbl showed that there is considerable variation in the general orientation of their respective side chains. This could be explained by the presence of van der Waals forces between the longer alkyl  $\beta$ -axial ligands (such as ethyl and butyl groups in EtCbl and BuCbl) with the side chains in the corrin ring, compared to the inability of the

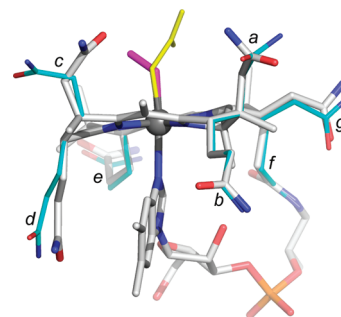


**Figure 6.** Superposition of the structures of EtCbl (white) and (NH<sub>2</sub>)<sub>2</sub>CSCbl (cyan). For clarity, only the seven amide side chains (labeled *a*–*g*) are shown for the (NH<sub>2</sub>)<sub>2</sub>CSCbl structure. The location of the bound ethyl (magenta) and (NH<sub>2</sub>)<sub>2</sub>CS (yellow) groups are also shown.

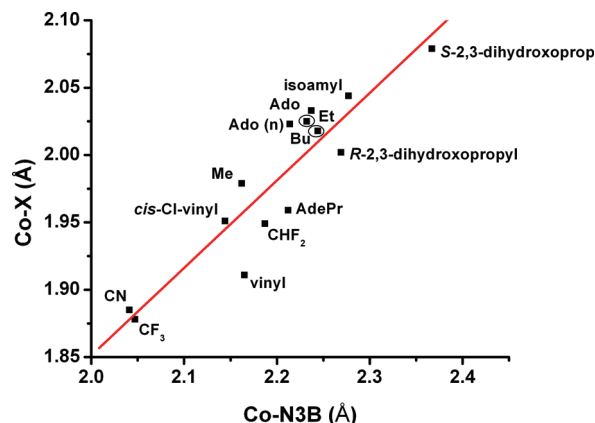


**Figure 7.** Plot of the axial Co–C against Co–N3B for Co–C bonded cobalamins. EtCbl and BuCbl are indicated with circled dots. The equation of linear regression is:  $0.552 + 0.649X$ ,  $r^2 = 0.919$ , ( $N = 14$ ).

methyl group in MeCbl to establish interactions with rather distant side chains projecting above and below the plane of the corrin ring.

It has been established that all alkylcobalamins display the so-called “inverse” *trans* influence,<sup>33</sup> where the distances of both axial ligands lengthen or shorten when the electron donating ability of the upper axial ligand (*R*) increases or decreases, respectively. EtCbl and BuCbl are no exception, as evidenced by comparison with other available structures (Table 3). A linear correlation ( $r^2 = 0.919$ ) was obtained by plotting Co–C versus Co–N3B bond distances for a number of alkylcobalamins, as shown in Figure 7. Lengthening of the Co–C bond in alkylcobalamins is thought to be a consequence of the steric repulsion caused by bulky  $\beta$ -axial ligands (such as ethyl and butyl groups), whereas lengthening of the Co–N3B bond appears to be electronic in nature, as a consequence of the strong  $\sigma$ -donation from the alkyl ligands.<sup>33</sup>

## Summary

The X-ray crystal structures of EtCbl and BuCbl were obtained with some of the lowest crystallographic residuals ( $R = 0.0468$  and  $0.0438$ , respectively), making full use of the high intensity X-rays from a synchrotron source. Both EtCbl and BuCbl exhibited an “inverse” *trans* influence, as depicted by the lengthening of their Co–C and Co–N3B bonds.

Analysis of the molecular surface maps showed that both alkyl ligands in EtCbl and BuCbl project toward the hydrophobic side of the corrin ring. Comparison with other cobalamins showed that in general the  $\beta$ -axial substituent is directed toward the hydrophobic side of the  $\beta$  face of the corrin somewhere between the C46 methyl and the C54 methyl groups. To that end, it has been proposed that the hydrophobic axial groups (methyl groups on C46 and C54 and the methylene groups of the *a* and *c* side chains) protect the reactive methyl or adenosyl groups in the coenzymes during catalytic turnover.<sup>26</sup> These findings together with the results presented herein strengthen the notion that very fine structural and conformational relationships must be involved in the biological roles of Nature's most beautiful cofactor.<sup>45</sup>

**Acknowledgment.** This research was funded by the National Heart, Lung and Blood Institute of the National Institutes of Health (HL71907 to D.W.J.) and Kent State University (N.E.B.). SSRL is a national user facility operated by Stanford University on behalf of the U.S. Department of Energy, Office of Basic Energy Sciences. The SSRL Structural Molecular Biology Program is supported by the Department of Energy (BES, BER) and by the National Institutes of Health (NCRR, BTP, NIGMS).

**Supporting Information Available:** Crystallographic data in CIF file format. This material is available free of charge via the Internet at <http://pubs.acs.org>.